

RELATION BETWEEN SIGNALS OF THE BEAM LOSS MONITORS AND RESIDUAL RADIATION IN THE J-PARC RCS

M. Yoshimoto[#], H. Harada, M. Kinsho, K. Yamamoto
 J-PARC, JAEA, Tokai, Ibaraki, 319-1195, Japan

Abstract

To achieve routine high power MW-class beam operation requires that the machine activations are within a permissible level. Thus, our focus has been to reduce and manage beam losses. Following the issues with the ring collimator in April 2016, the GM counter now measures the residual dose along the ring. These detailed dose distributions can now provide more details of the beam loss. Here, a new BLM is proposed that detects the spot area beam loss to determine the relation between the residual dose distribution and the beam loss signals. The new BLM will allow for a detailed map of the beam losses.

INTRODUCTION

The 3-GeV Rapid Cycling Synchrotron (RCS) of the Japan Proton Accelerator Research Complex (J-PARC) accelerates protons from 400 MeV to 3 GeV kinetic energy at 25 Hz repetition rate. The average beam current is 0.333 mA and the design beam power is 1 MW [1]. In addition, the RCS has two functions as a proton driver for neutron/muon production at the Material and Life science experimental Facility (MLF) and as a booster of the Main Ring synchrotron (MR) for the Hadron experimental facility (HD) and Neutrino experimental facility (NU). In order to maintain such routine high power MW-class beam operation, the machine activations must be kept within a permissible level. Therefore, we adopt a ring collimator system to remove the beam halo and localize the beam loss at the collimator area [2]. Fig. 1 shows the schematic view of the RCS ring and the ring collimator system. The RCS ring collimator system consists of a primary collimator, also referred to as “scatter”, which scatters the halo particles, and five secondary collimators, so-called “absorbers”, which absorb those scattered particles.

During April, 2016, the ring collimator system experienced serious trouble. A collimator control system failure occurred followed by a vacuum leak at the secondary collimator no. 5 (Col-Abs. no. 5). In order to restart the user beam operation, the Col-Abs. no. 5 was replaced with spare ducts, which did not have radiation shielding. In addition, as a precaution, every other collimator from this system must be stopped. As a result, it is difficult to maintain localization of the beam loss in the RCS after the restart of the beam operation. Therefore, a series of particle tracking experiments were carried out to examine how the particles were lost under various collimator arrangements. The change in the beam loss profile and variations in the radiation dose were estimated

in advance. After solving the problem with the collimator, we tried tuning the beam to minimize the beam loss without adjusting the collimator. Subsequently, the user beam operations are restarted [3]. In addition, we measured the residual dose along the ring every short maintenance period to investigate the influence of the collimator trouble.

In this paper, we report measurement results of the residual dose distribution along the ring. The relation between the residual dose distribution and the beam loss signals indicates new knowledge of the RCS beam loss sources and mechanism. In addition, we introduce a new beam loss monitor (new BLM), which detects the spot area beam loss to evaluate the residual radiation of the ring.

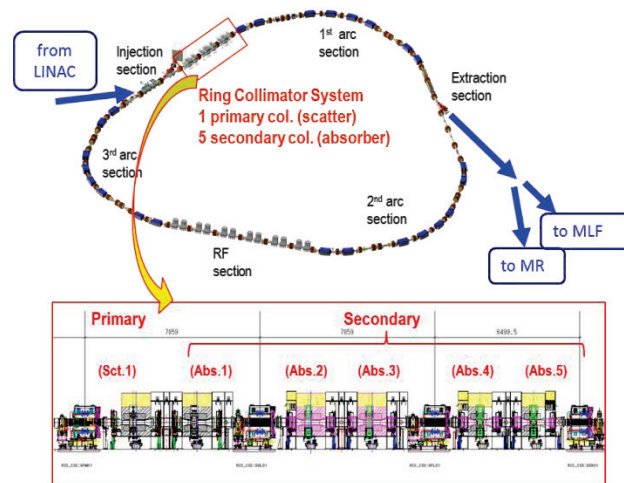


Figure 1: Schematic view of the Japan Proton Accelerator Research Complex (J-PARC) rapid cycling synchrotron (RCS) and the ring collimator system.

RESIDUAL DOSE MEASUREMENT

The beam loss profiles along the ring were predicted to change drastically due to the replacement of the Col-Abs. no. 5 with the spare ducts. Thus, detailed distributions of the residual dose along the ring were measured using a Geiger–Müller counter and compared with the distribution of the beam loss signals obtained by proportional counter-type beam loss monitors (P-BLMs). Fig. 2 shows the comparison between the beam loss signals and the residual dose distributions on four sides of the duct along the ring. The P-BLMs are installed along the ring and beam lines, and they are mainly used in the interlock system for machine protection [4]. The P-BLM signals are integrated and archived at every beam-shot. The RCS has a threefold symmetric lattice that partitions

[#] yoshimoto.masahiro@jaea.go.jp

into 27 FODO cells (three cells in each straight section and six cells in each arc section). Next, a few P-BLMs are placed in every cell with typical locations under the steering magnets as shown in Fig. 2. Therefore, it is difficult to obtain the definitive loss profile because the P-BLM is aimed at detecting significant beam loss at every cell. On the other hand, we measure the residual dose upstream and downstream of all bending magnets (BMs) and quadrupole magnets (QMs) in contact with inner, outer, upper, and lower sides of the each vacuum duct. In comparison with the P-BLM signals, the residual dose measurement results can indicate the detailed beam loss profiles in the ring and clearly distinguish the four side beam loss distributions. In particular, the inner side distribution exhibits a characteristic pattern. These results are stored in references to evaluate the influence of replacing the Col-Abs. no. 5 with the spare ducts. After the beam was tuned to minimize beam losses obtained by the P-BLMs, the user beam operation were restarted. Residual dose measurements were then carried out during every short maintenance period. The RCS operation status for every residual dose measurement is summarized in Table 1. A transition of the beam loss distribution during beam operation and transition of the residual dose distribution after the beam stop are shown in Fig. 3.

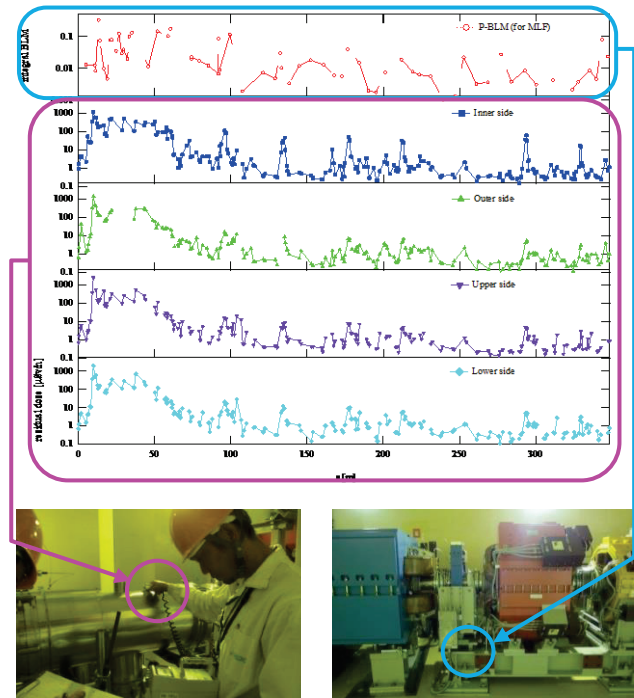


Figure 2: Comparison between the beam loss signals and the residual dose distributions along the four sides of the duct along the ring.

Table 1: Rapid cycling synchrotron (RCS) operation status for every residual dose measurement

	4/11	4/14	4/20	4/27
Operation period	Before restart	Half-day operation	One-week operation	Two-week operation
User (power)	MLF (205kW)	MLF (205kW) MR/NU (360kW)	MLF (205kW) MR/NU (385kW)	MLF (207kW) MR/NU (386kW)
Beam stop	4/4 7:00	4/14 7:45	4/20 9:00	4/27 9:00
Measurement	13:15–20:31	14:18–17:13	13:38–16:13	15:35–18:27
Elapsed time	174.3h–181.5h	6.5h–9.5h	4.5h–8.0h	6.5h–10h
Worker dose		0.05 mSv/h 0.01 mSv/h	0.09 mSv/h 0.02 mSv/h	0.13 mSv/h 0.03 mSv/h

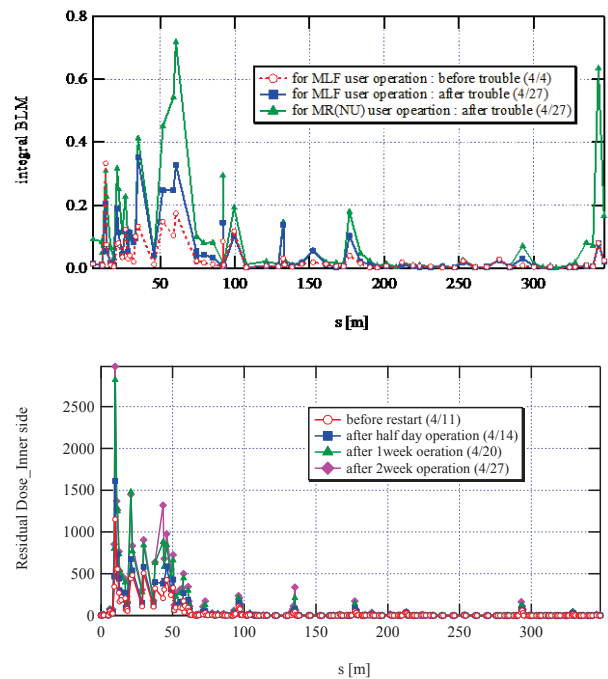


Figure 3: Influence of the spare ducts replacement of Col-Abs. no. 5. Upper plots show the comparison of the beam loss distributions before and after removing the Col. Abs. no. 5. Lower plots show the transition of the residual dose distributions after restarting the beam operation.

After restart of the user beam operation, the RCS was operated in two different modes according to the beam destinations. Thus, two beam loss profiles, not only for MLF user operation, but also MR/NU user operation, are measured independently. During MLF user operation, the beam losses increased by a factor of two. In addition, twice the amounts of beam loss for MLF are measured for MR/NU. The cause of the increase in beam loss is that an RCS beam power equivalent to 556 kW is needed to achieve the MR beam power of 360 kW. In either case, beam losses were expected during RCS operation. The reference residual dose was measured after a lapse of one

week from the beam stop. Recovering from the collimator trouble required some time because the radioactivity level of the Col-Abs. no. 5 was significantly high. On the other hand, residual dose measurement in every short maintenance period was carried out after about 6 h from the beam stop. Therefore, the lower plots in Fig. 3 refer to the compounding residual dose. From the plots, the MR/NU beam losses have very little influence on the residual dose compared to those for MLF since approximately 10% of the beam extracted from the RCS is transported to the MR and the remaining 90% is transported to the MLF.

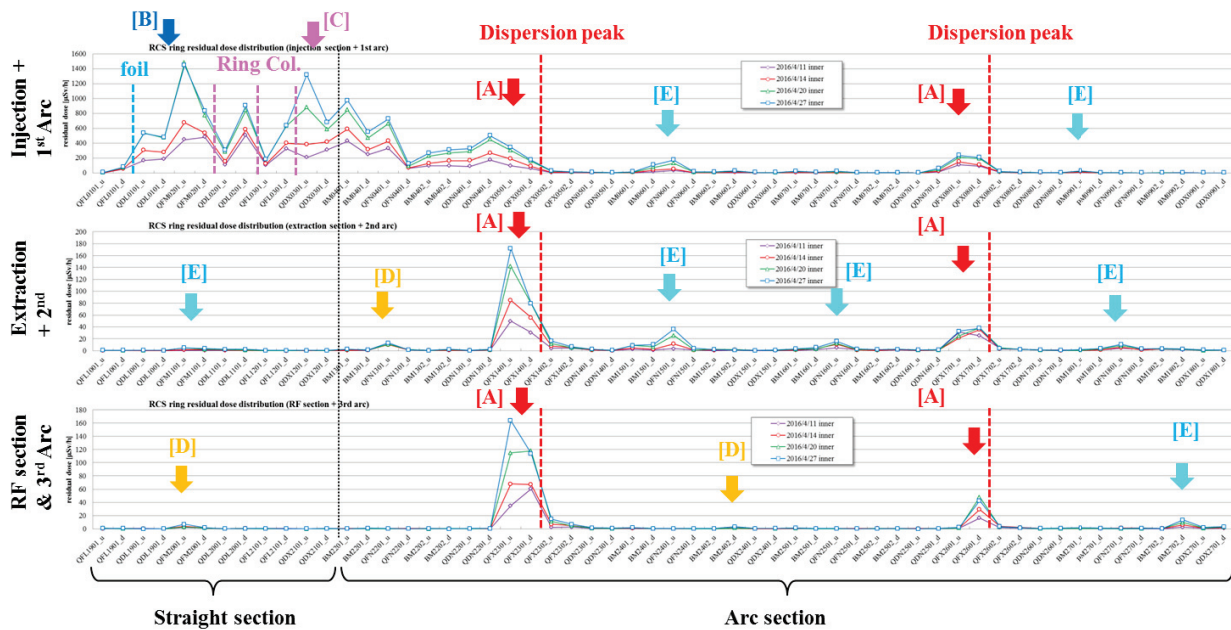


Figure 4: Transition of the measured residual dose distribution for the further study of the sources or the mechanism of the beam losses in the RCS ring.

In order to analyse the configuration of the beam loss profile, the transition of the measured residual dose is plotted as shown in Fig. 4. These distributions are divided into the three sections as related to the threefold symmetric lattice of the RCS. In addition, the horizontal axis changes from the position (s [m]) to the magnet ID. An auxiliary black straight line shows a boundary line between the straight section and the arc section, and red dotted lines show the dispersion peak positions. From the plots, there are some conspicuous beam loss structures and they can be classified into the five categories: [A], [B], [C], [D], and [E]. The beam losses categorized as [A] appear slightly above the dispersion peaks. These “dispersion peak beam losses” are caused by particle scattering and energy loss. The beam losses denoted as [B] appear at the injection area. These “injection beam losses” are caused by interactions with the stripper foil. In detail, there are two areas with high doses of radiation, and they are caused by different particles as follows: one appears above the ring collimator, caused by large angle scattering particles at the foils. To reduce this residual dose level, an additional collimator was installed, which

is referred to as an “H0 collimator,” at the H0 dump septum magnet [5]. However, the H0 collimator control system is adopts the same system as the ring collimators. Thus, adjustments between the beam and the H0 collimator cannot be done, and the beam losses increase after restarting the user beam operation. Since the collimator system upgrade was designed and tested, the beam losses can be minimized by adjusting the collimators after the summer-long maintenance period. The other appears around the stripper foil and it is caused by secondary particles due to nuclear reactions at the foil [6]. This radio-activation is an intrinsically serious problem for the RCS, which adopts the charge exchange multi-turn beam injection scheme with the stripper foil [7]. To reduce this radioactivity, we decreased the foil hitting rate by expanding the transverse painting area [8]. The beam losses denoted as [C] appear below the ring collimators. These “ring collimator beam losses” are caused by secondary particles generated in the ring collimators. The spare ducts exclude radiation shields, and subsequently secondary particles are leaked and radio-activated below the vacuum chambers. The spare

ducts are replaced with the straight vacuum duct with the radiation shielding. As a result, it is expected to reduce the “ring collimator beam losses” following the summer period. New Col-Abs no. 5 has been manufactured and is planned to be installed in the ring during the summer of 2017. The [D] beam losses appear at a few areas around the ring. These beam losses are small and the residual dose level is almost unchanged after restart. The cause is a long-lived nuclide that had been generated by the beam loss a long time ago, namely these beam losses have not occurred in these areas until now. The beam losses denoted as [E] also appear at a few areas around the ring, and these residual dose levels are not so high. However, they increase during user beam operation. From the beam tracking simulation, it is highly possible that the beam core particles are scattered by the secondary collimators and not the primary collimator, and then lost at unexpected aperture limits. Thus, these “absorber scattering beam losses” are not so high and cannot be detected by the beam loss monitor. However, they should be characterized as an important indicator of finer ring collimator adjustment.

SPOT AREAR BEAM LOSSES DETECTION WITH THE NEW-BLM

Transitions of the residual dose measured on the inner side and outer side along the spare ducts were measured as shown in Fig. 5. These beam losses are caused by the secondary particles generated by the ring collimators, and also denoted as [C]. However, there is a large residual dose imbalance between the inner and outer sides of the spare ducts. The reason for the dose imbalance is that the scatter or absorbers of the ring collimators lose their overall balance. Indeed, residual doses on the inner and outer copper block in the Col-Abs. no. 5 are 10 mSv/h and 40 mSv/h, respectively. On the other hand, the residual doses on the inner and outer copper block in the Col-Abs. no. 4 are 125 mSv/h and 10 mSv/h, respectively. Using the P-BLM, which detects significant beam loss at every cell, obtaining a finer symmetric adjustment of the scatters and absorbers horizontally and vertically is quite difficult. Therefore, to understand the horizontal and vertical balance of the beam loss, a new BLM that can detect the spot area beam loss is required. To meet these criteria, the scintillator is made smaller and fits on the duct directly. Accordingly, it can enhance the sensitivity to the beam loss generated at the contact area, and limit impact of the ones at a position relatively separated from the scintillator. The left photograph in Fig. 6 shows the new BLM. It is constructed with a small plastic scintillator (EJ-212, 20 mm × 20 mm × 50 mm) and a high-sensitivity photomultiplier tube (PMT: Hamamatsu H11934-100-10). After the connection, aluminum foil, used as a reflector, and shielding tape are wrapped on the scintillator. To investigate the scintillator’s performance, two new BLMs were installed on the inner and outer sides of the Ti reducer duct, which is a component of the spare ducts as shown in Fig. 6. Each PMT applies a negative

high voltage of -0.5 kV, and both outputs are connected directly to an oscilloscope via correctly terminated 50 Ohm. Typical measured raw signals are shown in Fig. 7. From the comparison results, a large imbalance of the beam losses is clearly detected. In addition, the inner and outer integrated values from the waveforms are 51 mVms and 125 mVms, respectively. On the other hand, the residual doses at the same place are 0.913 mSv/h and 2.23 mSv/h. The ratio of the integrated BLM signal is 51:125 and the ratio of the residual dose is 0.913:2.23. Both ratios are equal to the ratio 1:2.4, namely both experimental results are consistent.

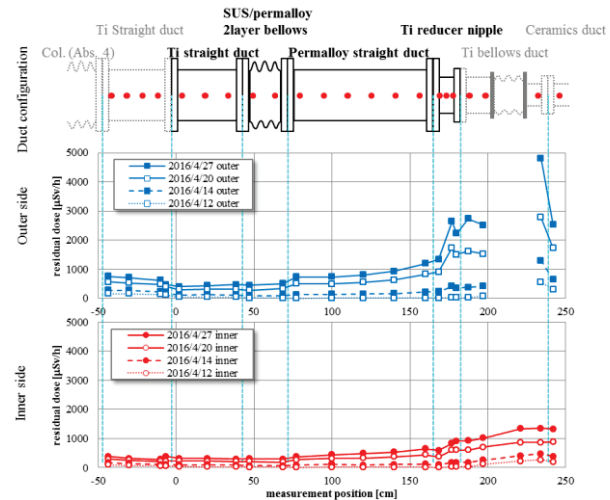


Figure 5: Comparison of the measured residual dose distributions between on the inner and outer sides along the spare ducts.

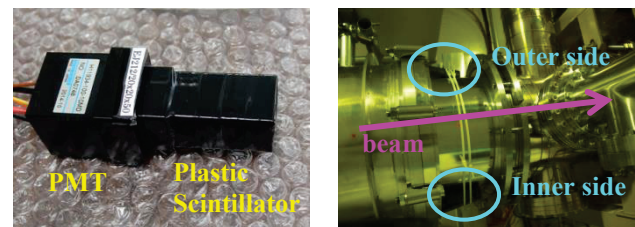


Figure 6: Photos of the new beam loss monitor (BLM) to detect the spot area beam losses (left), and installation of the two new BLMs on the inner and outer sides of the spare ducts (right).

After the beam stop during this summer shut down period, the radioactivity in the vacuum duct was measured using the new BLMs. The high PMT voltage increased up to the highest rated voltage of -0.9 kV to detect the gamma rays emitted from the vacuum duct. Two-second waveform data was acquired by means of the oscilloscope after changing the terminated resistor to 1 M Ohm and averaging offline. Radioactive decay curves obtained from the new BLM are plotted in Fig. 8. In addition, the residual dose measured by the GM counter at the near position is plotted in Fig. 8 to compare with the new BLM measurement results. From the comparison, relations between radioactivity and beam loss can be established.

Thus, we can evaluate the residual dose exactly by using the new BLM without the risk of exposure to the workers.

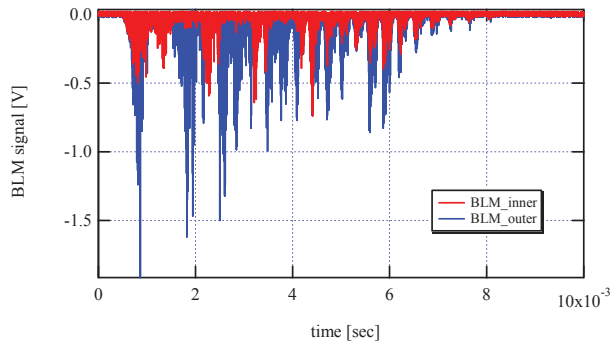


Figure 7: Typical measurement result of the new BPMs.

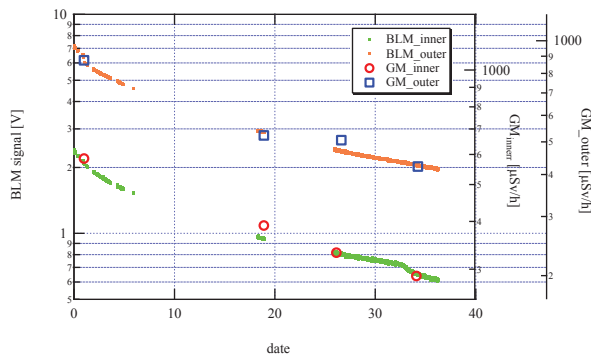


Figure 8: Decay curves of the radioactivity in the vacuum ducts obtained by the new BLM and residual dose at the near point measured by the GM counter.

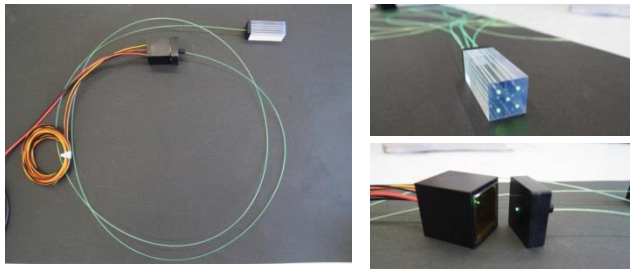


Figure 9: Assembly work of the upgraded new BLM. The photomultiplier tube (PMT) can be separated from the spot area of the beam losses to be connected with the plastic scintillator by the optical fibers.

If the detailed distribution of the residual dose is obtained by the new BLMs, many new BLMs should be set along the ring. In this case, they may be set near the magnet or inside the collimator shielding, and the magnetic field or the high level radiation should induce an operation error of the PMT. Thus, the new BLM will be upgraded to reduce some of the detrimental effects to the PMT. Therefore, the PMT is separated from the plastic scintillator and connected to it by optical fibers, as shown in Fig. 9. After the assembling work, offline analysis must be used to evaluate optical transmission line transition loss and waveform distortion. When the upgrade-BLM is

installed in the ring, an optical fiber connector, which is constructed with the PMT and optical fibers, is aligned along the upgrade-BLM. Background noise signals generated in the optical fibers themselves can be corrected by subtracting the connector signal from the upgrade-BLM signal.

SUMMARY

Following the ring collimator damages that occurred in April, 2016, the residual dose along the ring has been measured using a GM counter. The detailed residual dose distributions exhibit some conspicuous beam loss structures, and the classification of the beam loss structures provide us with further information of the beam loss. In particular, finding the absorber scattering beam losses is a milestone for finer ring collimator adjustment.

In order to establish the relation between the residual dose distribution and the beam loss signals, we developed and tested a new BLM, which can detect the spot area beam loss. In addition, we proposed an upgrade to the new BLM so that it can be used near the magnet and inside the collimator shielding. It is expected that a detailed map of beam losses can be obtained using the new BLM.

REFERENCES

- [1] High-intensity Proton Accelerator Project Team, JAERI Report No. JAERI-Tech 2003-044 and KEK Report No. 2002-13.
- [2] K. Yamamoto, “Efficiency simulations for the beam collimation system of the Japan Proton Accelerator Research Complex rapid-cycling synchrotron”, PRST-AB 11, 123501 (2008).
- [3] K. Yamamoto *et al.*, “A malfunction of the beam collimator system in j-parc 3 gev rapid cycling synchrotron”, in Proc. of PASJ2013, MOP007 (in Japanese).
- [4] K. Yamamoto, “Signal response of the beam loss monitor as a function of the lost beam energy”, Proc. of IBIC2015, Melbourne, Australia (2015), MOPB021.
- [5] S. Kato *et al.*, “Localization of the large-angle foil-scattering beam loss caused by the multiturn charge-exchange injection”, PRST-AB 16, 071003 (2013)
- [6] M. Yoshimoto *et al.*, “Maintenance of radio-activated stripper foils in the 3 GeV RCS of J-PARC”, JRNC, 3, 305 (2015), PP 865-873.
- [7] E. Yamakawa *et al.*, “Measurements and PHITS Monte Carlo Estimations of Residual Activities Induced by the 181 MeV Proton Beam in the Injection Area at J-PARC RCS Ring”, JPS Conf. Proc. 8, 012017 (2015).